Civil Engineering Dimension
https://ced.petra.ac.id

Performance Evaluation of Simple Regular Buildings using FBD and DDBD Methods with a Consistent Target Drift

Pudjisuryadi, P.[1]*, Sumargo, W.[1], Kho, A.[1], and Lumantarna, B.[1]
[1] Faculty of Civil Engineering and Planning, Civil Engineering Department, Petra Christian University
Jl. Siwalankerto 121-131, Surabaya 60236, INDONESIA

DOI: https://doi.org/10.9744/ced.27.1.59-72

Article Info:
Submitted: Feb 28, 2025
Reviewed: Mar 04, 2025
Accepted: Mar 11, 2025

Keywords:
Direct Displacement Based Design,
Force Base Design,
drift,
nonlinear analysis,
Reinforced Concrete Structure.

Corresponding Author:
Pudjisuryadi, P.
Faculty of Civil Engineering and Planning,
Civil Engineering Department,
Petra Christian University,
Jl. Siwalankerto 121-131, Surabaya 60236,
INDONESIA
Email: pamuda@petra.ac.id

Abstract

The Direct Displacement Based Design (DDBD) method, proposed by Priestley, is an alternative to the traditional Force-Based Design (FBD) method for earthquake-resistant design. This study compares the performance of 4-story and 12-story buildings designed using both FBD and DDBD with the same target drift of 2%. The differences in base shear used for the design of the two approaches are discussed. To evaluate the buildings' performance, Nonlinear Dynamic Procedure (NDP) analysis, or nonlinear time history analysis, was conducted considering 500 and 2500 years return period earthquakes. The results indicate that the actual drift of both designs deviates from the target drift; however, the observed drifts remain within the maximum limits set by FEMA 356. Moreover, plastic damages were observed in unexpected areas of the columns, suggesting that the strong-column weak-beam design concept, as stipulated by building codes, does not entirely prevent damage to columns.

INTRODUCTION

Seismic design concepts can be classified into Force Based Design (FBD) and Displacement Based Design (DBD). Although improvements are ongoing [1-3], FBD is more widely adopted across design codes, including the Indonesian standard SNI 03-1726-2019 [4]. In contrast, DBD is still under development [5-6], with one notable method, Direct Displacement-Based Design (DDBD), proposed by Priestley et al. [7] in 2007. As the name suggests, DDBD focuses on ensuring that a structure does not exceed a predefined displacement target when subjected to a target earthquake. After DDBD was first introduced, researchers began evaluating the performance of structures designed with DDBD, applying it to various types of structures. Sadan et al. [8] and Cademartori et al. [9] assessed existing bridge structures using DDBD and yielded accurate results. Dong et al. [10] extended the application of DDBD to glulam structures with buckling restrained braces in 3-, 6-, and 9-story buildings, finding them effective in resisting lateral earthquake forces. However, Chikmath et al. [11] observed that a 12-story reinforced concrete frame designed using DDBD exhibited a drift ratio exceeding the allowable inter-story drift limit, suggesting that DDBD may not be ideal for buildings where the fundamental mode is not dominant. Furthermore, there has been growing interest in comparing the performance of DDBD with FBD, which is more commonly used. Muljati et al. [12] conducted a comparative study of structures designed using the Indonesian code SNI 03-1726-2019 (FBD) and DDBD. The study [12] concluded that buildings designed with DDBD often result in larger dimensions than those designed with FBD.

Note : Discussion is expected before July, 1st 2025, and will be published in the "Civil Engineering Dimension", volume 27, number 2, September 2025.
ISSN : 1410-9530 print / 1979-570X online
Published by : **Petra Christian University**

This study aims to further investigate the factors that may contribute to the differences between FBD and DDBD. It aids engineers in recognizing design factors that are more sensitive to the results, enabling them to exercise greater care when determining values that rely on engineering judgment. A comparison is made between the design concepts and assumptions underlying both methods. Two reinforced concrete buildings, with 4 and 12 stories, were designed using both methods and serve as case studies for the analysis. The buildings' performance was evaluated using nonlinear dynamic procedures (nonlinear time history analysis). A brief overview of the DDBD method is presented in the followings.

Direct Displacement based Design (DDBD) Method

DDBD method determines the earthquake load on a building based on a target displacement (Δ_d) that the structure aims to achieve during its final phase of deformation [2]. Initially, the structure is idealized as a single-degree-of-freedom (SDOF) system, characterized by its effective height (H_e), effective mass (m_e), and effective stiffness (K_e). Structural equivalent damping (ξ_{eq}) which is a combination of elastic damping (5%) and hysteretic damping, is determined depending on the type of structure. A reduction factor (R_ξ) is then calculated based on the target displacement and damping characteristics. This reduction factor is applied to derive the displacement response spectrum corresponding to the structural damping. From the spectrum, the effective period (T_e) of the structure is determined. Subsequently, the effective stiffness and total base shear (V_{base}) can be calculated. Figure 1 summarizes the conceptual framework of the DDBD method.

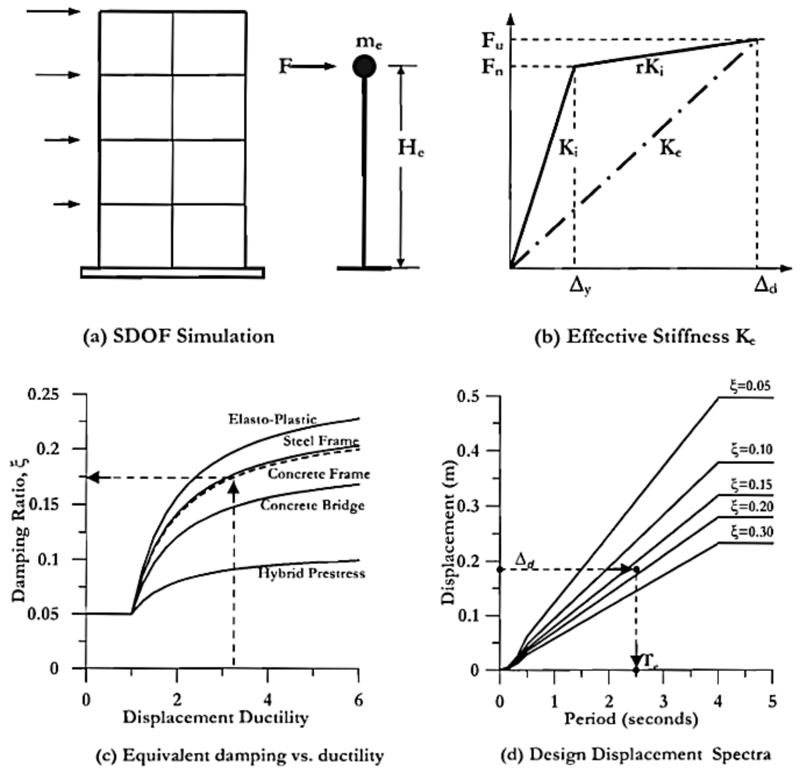

Figure 1. Direct Displacement based Design Concept [7]

For multi-degree-of-freedom (MDOF) structures, such as frames, the step-by-step DDBD procedure for calculating the total base shear (V_{base}) is as follows:

Step 1. Develop an Equivalent SDOF system
An equivalent SDOF system is derived from the MDOF system, as illustrated in Figure 2. In the figure, d_i represents the inelastic mode shape, defined by Equations 1 and 2, where n is the number of floors, H_n is the height of the structure, and H_i is the elevation of the i^{th} floor. The displacement of the i^{th} floor (D_i) is given by Equation 3, where D_c and d_c are the design displacement and value of the mode shape at the critical mass c, respectively. The target displacement can then be calculated using Equation 4, where m_i is the mass of the i^{th} floor. The effective mass (m_e) and effective height (H_e) of the SDOF system can be determined using Equations 5 and 6.

$$n \leq 4 : \delta_i = \frac{H_i}{H_n} \tag{1}$$

$$n > 4: \ \delta_i = \frac{4}{3}(\frac{H_i}{H_n})(1 - \frac{H_i}{4H_n}) \tag{2}$$

$$\Delta_i = \delta_i(\frac{\Delta_c}{\delta_c}) \tag{3}$$

$$\Delta_d = \sum_{i=1}^{n}(mi \ \Delta_i^2) \,/\, \sum_{i=1}^{n}(mi \ \Delta_i) \tag{4}$$

$$m_e = \sum_{i=1}^{n}(mi \ \Delta_i) \,/\Delta_d \tag{5}$$

$$H_e = \sum_{i=1}^{n}(mi \ \Delta_i \ H_i) \,/\, \sum_{i=1}^{n}(mi \ \Delta_i) \tag{6}$$

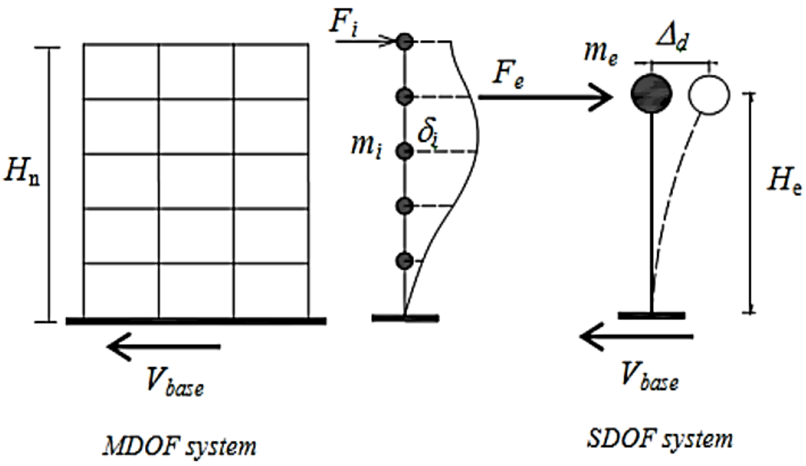

Figure 2. Equivalent SDOF System [7]

Step 2. Estimate the Equivalent Viscous Damping (x_{eq})
For a frame, the equivalent viscous damping (x_{eq}) is calculated using Equations 7 and 8, where m and D_y represent the ductility and yield displacement, respectively. The yield displacement is estimated from the effective height (H_e), yield moment (M), and yield rotation (q_y) of the beams, as calculated from Equation 9, where b is the number of bays in the frame. The beam yield rotation depends on the beam's length (L_B), section height (H_B), and its reinforcement yield strain (e_y), as given by Equation 10.

$$\xi_{eq} = 0.05 + 0.565(\frac{\mu - 1}{\mu\pi}) \tag{7}$$

$$\mu = \frac{\Delta_d}{\Delta_y} \tag{8}$$

$$\Delta_y = \frac{\sum_{i=1}^{b} M_i \theta_{yi}}{\sum_{i=1}^{b} M_i} H_e \tag{9}$$

$$\theta_y = 0.5\varepsilon_y \frac{L_B}{H_B} \tag{10}$$

Step 3. Determine the Effective Period (T_e)
From the acceleration design spectrum, a displacement design spectrum is developed for the SDOF system with damping equal to the equivalent viscous damping (x_{eq}). Given the target displacement (D_d), the effective period (T_e) can be determined (see Figure 1d).

Step 4. Calculate the Effective Stiffness (K_e) and the Total Base Shear (V_{base})
The effective stiffness (K_e) and total base shear (V_{base}) are calculated using Equations 11 and 12.

$$K_e = (\frac{2\pi}{Te})^2 m_e \tag{11}$$

$$V_{base} = K_e \ \Delta_d \tag{12}$$

The Case Studies

The key variable used for comparison between the two design methods is the target displacement. The dimensions of the structural elements are determined such that the nonlinear displacement of the building designed using the

FBD method (estimated by multiplying the elastic displacement by C_d, the deflection amplification factor) is the same as the target displacement set in the DDBD method. In this study, an inter-story drift ratio of 2% was selected to determine the target displacement.

As mentioned previously, two buildings (4- and 12-story) of a typical floor plan, as shown in Figure 3(a), were designed for a site in Surabaya with a site class E. The typical story height is 4 meter, resulting in overall building heights of 16 meters for the 4-story building and 48 meters for the 12-story building. The corresponding basic elastic design response spectrum is presented in Figure 3(b). In the FBD method, a special moment-resisting frame is selected as the seismic resisting system, with concrete and steel strengths of 25 MPa and 420 MPa, respectively. The gravity loads considered in this study consist of self-weight of the structure, superimposed dead load, and live load. A live load of 2.4 kN/m^2 [13] was applied to all floors because the building is assumed as an office. A superimposed dead load of 1.5 kN/m^2 was applied to all stories. Using the equivalent static force procedure [4], the resulting element dimensions required to achieve the 2% story drift ratio are presented in Table 1. These dimensions were subsequently used for buildings designed using the DDBD approach.

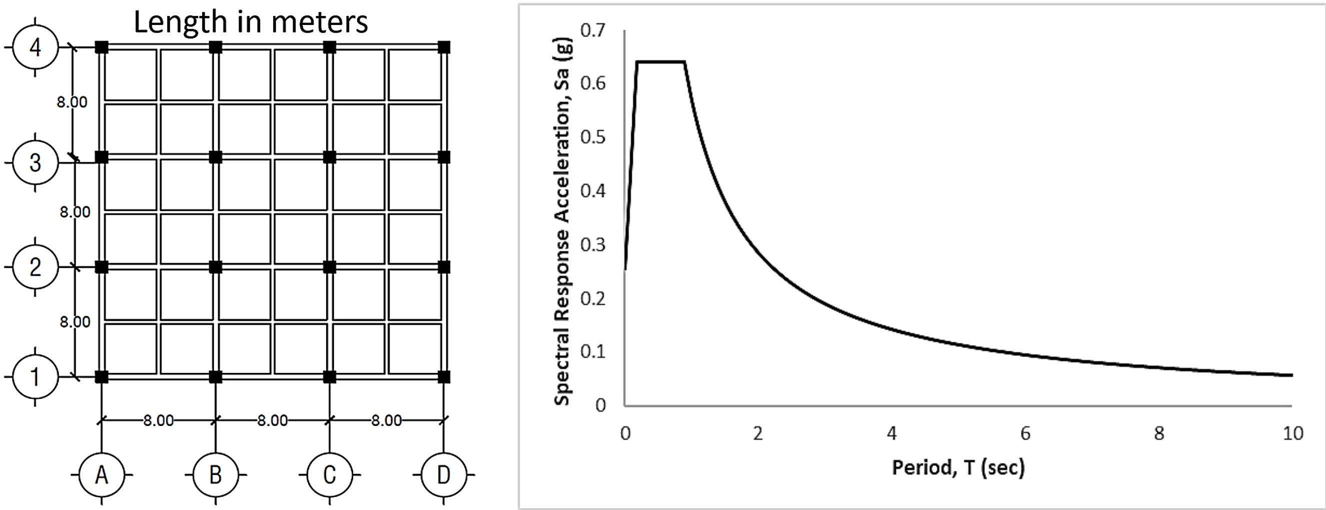

(a) (b)

Figure 3. (a) Building Plan, (b) Basic Elastic Design Response Spectrum

Table 1. Beam and Column Dimensions used for FBD and DDBD approaches

Story	4-Story			12-Story		
	Main Beam (mm)	Secondary Beam (mm)	Column (mm)	Main Beam (mm)	Secondary Beam (mm)	Column (mm)
1	400x650	300x550	650x650	400x900	300x550	1200x1200
2	400x650	300x550	650x650	400x900	300x550	1200x1200
3	400x650	300x550	650x650	400x900	300x550	1200x1200
4	400x650	300x550	650x650	400x900	300x550	1200x1200
5	-	-	-	400x900	300x550	1000x1000
6	-	-	-	400x900	300x550	1000x1000
7	-	-	-	400x900	300x550	1000x1000
8	-	-	-	400x900	300x550	1000x1000
9	-	-	-	400x900	300x550	800x800
10	-	-	-	400x900	300x550	800x800
11	-	-	-	400x900	300x550	800x800
12	-	-	-	400x900	300x550	800x800

Variables and Assumptions for Each Method

Both FBD and DDBD methods involve several variables (Table 2) that must be determined. It is important to note that the assumed values for these variables can significantly influence the resulting earthquake loads. Thus, a direct comparison between the two methods can be challenging. Table 3 provides the values of these variables as utilized in this study.

Table 2. Determination of Key Variables of FBD and DDBD Methods

Variable	FBD	DDBD
Importance Factor	Depending on the building risk category given in Table 3 of SNI 1726:2019 [4]	Not a design variable
Mode Shape	Not a design variable	An inelastic mode shape is assumed (Priestley et al. [7]) to determine the design displacement (Δ_d).
Effective mass (m_e), Effective height (H_e), Target Displacement (Δ_d) Yield Displacement (Δ_y)	Not a design variables	Calculated from equations by Priestley et al. [7]
Structural Ductility (μ)	The maximum response modification coefficient (R), which is a function of ductility, is given in Table 12 of SNI 1726:2019 [4]	Design ductility is determined from Δ_d/Δ_y
Structural Damping	An elastic damping of 5% is assumed	Using a combination of 5% elastic damping and additional hysteresis damping based on the type of structure [7].
Story Shear Distribution	Determined by empirical equations based on the seismic weight and elevation of each floor [4]	Determined by empirical equations based on the story mass (m_i) and story target displacement ($\square_i$)
Structural Analysis	Standard finite element analysis	Simplified approach [7]

Table 3. Values of the Key Variables Used/Calculated in this Study

Variable	FBD		DDBD	
	4-story	12-story	4-story	12-story
Importance factor (I_e)	1	1	-	-
Effective mass (m_e) (ton)	-	-	1851.75	6640.74
Effective height (H_e) (m)	-	-	11.903	31.67
Design displacement (Δ_d) (m)	-	-	0.238	0.444
Yield displacement (Δ_y) (m)	-	-	0.169	0.325
Structural ductility (μ)	5	5	1.406	1.592
Structural damping ($\square_{eq}$)	5%	5%	10.20%	11.69%

Total Base Shear and Story Shear of the Buildings

With different values of the previously mentioned variables, it is expected that the resulting total base shear and distributed story shear, will differ between the two methods, as shown in Table 4. In this study, the resulting base shear forces differ by approximately a factor of two.

Table 4. Total Base Shear and Story Shear of the Buildings

Story	Story Shear, F_i (kN)			
	FBD-4	DDBD-4	FBD-12	DDBD-12
12	-	-	783.38	1661.79
11	-	-	714.34	896.58
10	-	-	590.36	837.1
9	-	-	478.19	773.22
8	-	-	392.02	731.39
7	-	-	312.91	683.89
6	-	-	229.9	600.49
5	-	-	159.65	512.32
4	922.17	1500.11	106.65	437.75
3	551.03	1195.16	62.86	351.82
2	244.9	796.77	27.94	239.76
1	61.23	398.39	6.98	122.49
Base Shear	1779.33	3890.42	3865.18	7848.6

Longitudinal Reinforcement for Beams and Columns

Tables 5 and 6 illustrate the longitudinal reinforcement for the beams and columns of the 4-story building, respectively, while Tables 7 and 8 provide the corresponding details for the 12-story building.

Table 5. Beam Reinforcement for 4-Story Building

Story	Location	Dimension (mm)	Rebar Position	Longitudinal Rebar (reinforcement ratio)	
				FBD	DDBD
4	interior	400 x 650	top	5D22 (0.81%)	3D22 (0.49%)
			bottom	3D22 (0.49%)	3D22 (0.49%)
	exterior		top	7D16 (0.6%)	3D22 (0.49%)
			bottom	4D16 (0.34%)	3D22 (0.49%)
3	interior		top	7D22 (1.15%)	4D22 (0.65%)
			bottom	4D22 (0.65%)	4D22 (0.65%)
	exterior		top	5D22 (0.81%)	4D22 (0.65%)
			bottom	3D22 (0.49%)	4D22 (0.65%)
2	interior		top	7D22 (1.15%)	5D22 (0.81%)
			bottom	4D22 (0.65%)	5D22 (0.81%)
	exterior		top	5D22 (0.81%)	5D22 (0.81%)
			bottom	3D22 (0.49%)	5D22 (0.81%)
1	interior		top	7D22 (1.15%)	6D22 (0.97%)
			bottom	4D22 (0.65%)	6D22 (0.97%)
	exterior		top	5D22 (0.81%)	6D22 (0.97%)
			bottom	3D22 (0.49%)	6D22 (0.97%)

Table 6. Columns Reinforcement for 4-Story Building

Story	Location	Dimension (mm)	Longitudinal Rebar (reinforcement ratio)	
			FBD	DDBD
4	Interior	650 x 650	12D22 (1.08%)	20D22 (1.8%)
	Exterior		8D25 (0.93%)	16D22 (1.44%)
	Corner		8D25 (0.93%)	8D22 (0.72%)
3	Interior		12D19 (0.81%)	20D22 (1.8%)
	Exterior		8D22 (0.72%)	20D22 (1.8%)
	Corner		8D19 (0.54%)	12D22 (1.08%)
2	Interior		12D19 (0.81%)	24D22 (2.16%)
	Exterior		8D25 (0.93%)	20D22 (1.8%)
	Corner		8D25 (0.93%)	12D22 (1.08%)
1	Interior		12D25 (1.39%)	28D22 (2.52%)
	Exterior		12D25 (1.39%)	20D22 (1.8%)
	Corner		12D25 (1.39%)	12D22 (1.08%)

Table 7. Beam Reinforcement for 12-Story Building

Story	Location	Dimension (mm)	Rebar Position	Longitudinal Rebar (reinforcement ratio)	
				FBD	DDBD
12	interior	400 x 900	top	4D22 (0.45%)	5D16 (0.3%)
			bottom	2D22 (0.23%)	5D16 (0.3%)
	exterior		top	8D13 (0.32%)	5D16 (0.3%)
			bottom	4D13 (0.16%)	5D16 (0.3%)
11	interior		top	5D22 (0.57%)	3D22 (0.34%)
			bottom	3D22 (0.34%)	3D22 (0.34%)
	exterior		top	4D22 (0.45%)	3D22 (0.34%)
			bottom	2D22 (0.23%)	3D22 (0.34%)
10	interior		top	6D22 (0.68%)	4D22 (0.45%)
			bottom	3D22 (0.34%)	4D22 (0.45%)
	exterior		top	5D22 (0.57%)	4D22 (0.45%)
			bottom	3D22 (0.34%)	4D22 (0.45%)
9	interior		top	7D22 (0.8%)	5D22 (0.57%)
			bottom	4D22 (0.45%)	5D22 (0.57%)
	exterior		top	6D22 (0.68%)	5D22 (0.57%)
			bottom	4D22 (0.45%)	5D22 (0.57%)
8	interior		top	7D22 (0.8%)	6D22 (0.68%)
			bottom	4D22 (0.45%)	6D22 (0.68%)
	exterior		top	6D22 (0.68%)	6D22 (0.68%)
			bottom	4D22 (0.45%)	6D22 (0.68%)

Story	Location	Dimension (mm)	Rebar Position	Longitudinal Rebar (reinforcement ratio)	
				FBD	DDBD
7	interior	400 x 900	top	8D22 (0.92%)	7D22 (0.8%)
			bottom	4D22 (0.45%)	7D22 (0.8%)
	exterior		top	7D22 (0.8%)	7D22 (0.8%)
			bottom	5D22 (0.57%)	7D22 (0.8%)
6	interior		top	8D22 (0.92%)	7D22 (0.8%)
			bottom	5D22 (0.57%)	7D22 (0.8%)
	exterior		top	7D22 (0.8%)	7D22 (0.8%)
			bottom	5D22 (0.57%)	7D22 (0.8%)
5	interior		top	8D22 (0.92%)	8D22 (0.92%)
			bottom	5D22 (0.57%)	8D22 (0.92%)
	exterior		top	7D22 (0.8%)	8D22 (0.92%)
			bottom	5D22 (0.57%)	8D22 (0.92%)
4	interior		top	8D22 (0.92%)	8D22 (0.92%)
			bottom	5D22 (0.57%)	8D22 (0.92%)
	exterior		top	7D22 (0.8%)	8D22 (0.92%)
			bottom	5D22 (0.57%)	8D22 (0.92%)
3	interior		top	7D22 (0.8%)	9D22 (1.04%)
			bottom	4D22 (0.45%)	9D22 (1.04%)
	exterior		top	6D22 (0.68%)	9D22 (1.04%)
			bottom	5D22 (0.57%)	9D22 (1.04%)
2	interior		top	6D22 (0.68%)	9D22 (1.04%)
			bottom	3D22 (0.34%)	9D22 (1.04%)
	exterior		top	5D22 (0.57%)	9D22 (1.04%)
			bottom	4D22 (0.45%)	9D22 (1.04%)
1	interior		top	5D22 (0.57%)	9D22 (1.04%)
			bottom	3D22 (0.34%)	9D22 (1.04%)
	exterior		top	4D22 (0.45%)	9D22 (1.04%)
			bottom	2D22 (0.23%)	9D22 (1.04%)

Table 8. Columns Reinforcement for 12-Story Building

Story	Location	Dimension (mm)	Longitudinal Rebar (reinforcement ratio)	
			FBD	DDBD
12	Interior	800x800	8D25 (0.61%)	16D25 (1.23%)
	Exterior		8D22 (0.48%)	12D25 (0.92%)
	Corner		8D22 (0.48%)	8D22 (0.48%)
11	Interior		8D25 (0.61%)	16D25 (1.23%)
	Exterior		8D25 (0.61%)	12D25 (0.92%)
	Corner		8D19 (0.35%)	8D25 (0.61%)
10	Interior		8D25 (0.61%)	20D25 (1.53%)
	Exterior		12D22 (0.71%)	16D25 (1.23%)
	Corner		8D22 (0.48%)	8D25 (0.61%)
9	Interior		8D22 (0.48%)	24D25 (1.84%)
	Exterior		12D22 (0.71%)	20D25 (1.53%)
	Corner		8D22 (0.48%)	12D25 (0.92%)
8	Interior	1000 x 1000	8D13 (0.11%)	20D25 (0.98%)
	Exterior		12D19 (0.34%)	16D25 (0.79%)
	Corner		8D22 (0.3%)	8D25 (0.39%)
7	Interior		8D13 (0.11%)	24D25 (1.18%)
	Exterior		8D22 (0.3%)	16D25 (0.79%)
	Corner		8D22 (0.3%)	12D22 (0.46%)
6	Interior		8D13 (0.11%)	24D25 (1.18%)
	Exterior		8D22 (0.3%)	20D25 (0.98%)
	Corner		8D22 (0.3%)	12D22 (0.46%)
5	Interior		8D13 (0.11%)	24D25 (1.18%)
	Exterior		8D22 (0.3%)	20D25 (0.98%)
	Corner		8D22 (0.3%)	12D22 (0.46%)
4	Interior	1200 x 1200	12D13 (0.11%)	20D25 (0.68%)
	Exterior		12D13 (0.11%)	16D25 (0.55%)
	Corner		12D19 (0.24%)	12D22 (0.32%)

Story	Location	Dimension (mm)	Longitudinal Rebar (reinforcement ratio)	
			FBD	DDBD
	Interior		12D13 (0.11%)	20D25 (0.68%)
3	Exterior		12D16 (0.17%)	16D25 (0.55%)
	Corner		12D25 (0.41%)	12D22 (0.32%)
	Interior		12D13 (0.11%)	20D25 (0.68%)
2	Exterior	1200 x 1200	12D22 (0.32%)	16D25 (0.55%)
	Corner		16D25 (0.55%)	12D22 (0.32%)
	Interior		12D16 (0.17%)	20D25 (0.68%)
1	Exterior		20D22 (0.53%)	16D25 (0.55%)
	Corner		20D29 (0.92%)	12D19 (0.24%)

Performances of the Buildings

The performances of the designed buildings were evaluated using nonlinear time history analysis. Ground acceleration records from the 1940 El-Centro and the 1995 Kobe - Chihaya Station earthquakes (Figure 4) are used as input for the analysis. These original ground motions were modified to match the response spectrum of Surabaya City. The buildings were subjected to two levels of seismic loading: the Basic Design Earthquake (BDE) and the Maximum Considered Earthquake (MCE_R). Ground motions were applied along two orthogonal directions, with intensities set at 100% in the N-S direction and 30% in the E-W direction. The parameters considered in evaluating structural performance were story drift ratio, damage level, and structural failure mechanism.

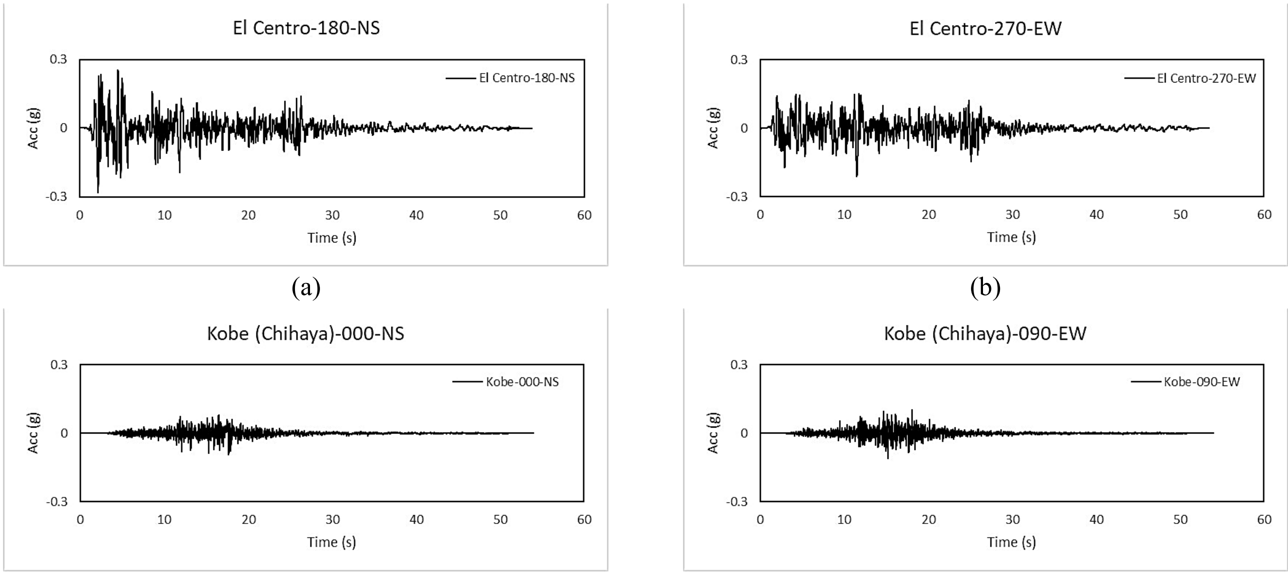

Figure 4. Ground Motion Record of: (a) El-Centro 1940 N-S, (b) El-Centro 1940 E-W, (c) Kobe 1995 Chihaya Station N-S, (d) Kobe 1995 Chihaya Station E-W [14]

Drift Ratio

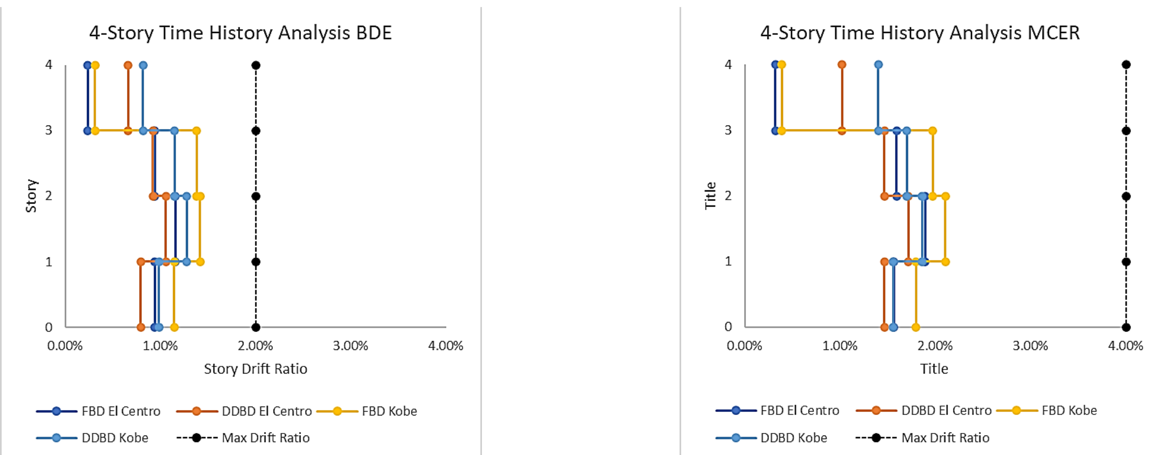

Figure 5. Inter Story Drift Ratio of 4-Story Building: (a) BDE, (b) MCE_R

The inter-story drift ratios for the 4-story and 12-story buildings are presented in Figures 5 and 6. According to FEMA 356 [15], for earthquakes with 10% and 2% probability of exceedance in 50 years (the BDE and MCE_R, respectively), the inter-story drift ratios are limited to 2% and 4%. The results indicate that all inter-story drift ratios remain within their respective limits. The maximum inter-story drift ratio values are summarized in Table 9.

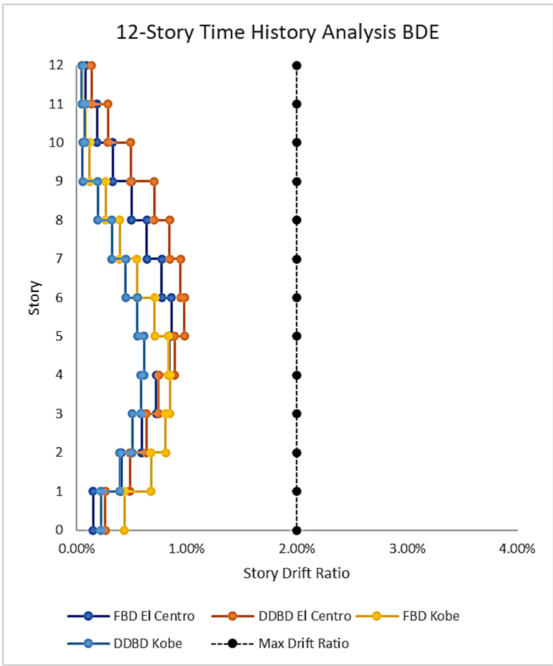

(a)

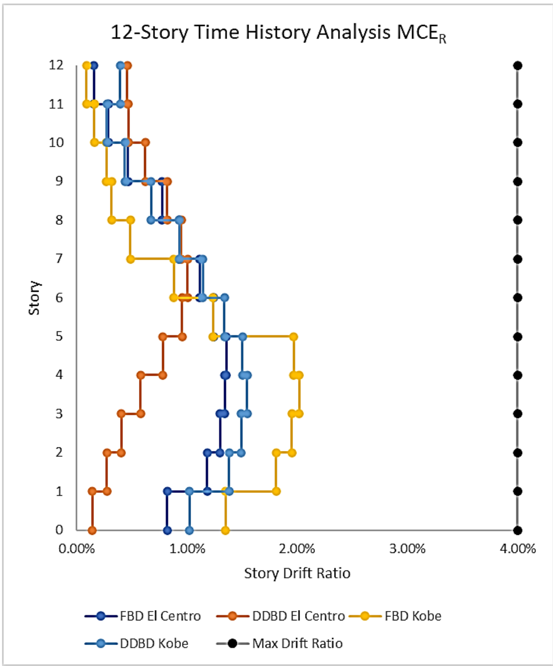

(b)

Figure 6. Inter Story Drift Ratio of 12-Story Building: (a) BDE, (b) MCE_R

Table 9. Maximum Inter Story Drift Ratio of Each Building

Building	BDE		MCE_R	
	El Centro	Kobe	El Centro	Kobe
4-FBD	1.16%	1.42%	1.89%	2.11%
4-DDBD	1.06%	1.27%	1.72%	1.86%
12-FBD	0.86%	0.85%	1.36%	2.02%
12-DDBD	0.98%	0.61%	1.01%	1.55%

Damage Level and Failure Mechanism

All buildings are expected to have a safe beam side sway mechanism, where controlled plastic damage might occur at the beam ends and the bottom of the first-floor columns. However, the results indicate that plastic damage also occurs in columns at other locations. In this study, the level of plastic damage is adopted from FEMA 356 [15] and presented in Figure 7 and Table 10.

In Figure 8, it can be seen that for 4-story buildings designed with both approaches and subjected to the El Centro earthquake at the BDE level, plastic damages have already occurred in some columns. These damages are in the very early stage, indicated by pink color (Stage B, see Table 10). With a higher level earthquake (Figure 9), the MCE_R, the damages become more severe, with buildings designed using the FBD approach experiencing column damage up to the Life Safety stage (cyan color). Similar results are observed for 4-story buildings subjected to the Kobe earthquake (Figures 10 and 11). Again, the damages are more severe in buildings designed using the FBD approach (smaller base shear), with column damage reaching the Immediate Occupancy stage (dark blue color) at the MCE_R level. As for the beams, as expected, plastic damages were observed, with a maximum of Life Safety stage for buildings designed using the FBD approach and Immediate Occupancy stage for those designed using the DDBD approach.

In Figure 12, the 12-story buildings designed with both approaches and subjected to the El Centro earthquake at the BDE level show plastic damages in some columns up to the Collapse Prevention stage (green color). With a higher level earthquake (Figure 13), the MCER, more plastic damages entered the Collapse Prevention stage, but none went beyond (failure). Figures 14 and 15 show similar results for 12-story buildings subjected to the Kobe earthquake.

Damages to the beams and columns of buildings designed with the FBD approach entered the Life Safety and Collapse Prevention stages, respectively. The beams of buildings designed with the DDBD approach showed slightly less damage, experiencing only the Immediate Occupancy stage.

Strong Column Weak Beam (SCWB) concept is applied during the design stage. However, the SCWB approach from Priestley is different from the SNI SCWB standard. Priestley's SCWB concept uses simplified formulas to determine the column design moment, but the results indicate that this approach is less effective, as many columns fail before the beams.

Tables 11 and 12 summarize the analysis results. In these tables, the "Mechanism" is marked with "OK" if the plastic damage occurs as expected, the "Damage Level" is marked with "OK" if the maximum plastic damage conditions are within the "Life Safety" and "Collapse Prevention" for BDE and MCE_R, respectively, and the “Drift Ratio” is marked with “OK” if its value does not exceed the specified limit.

Table 10. Plastic Hinge Color and State by FEMA 356 [15]

	Plastic Hinge State
B	B
IO	Immediate Occupancy
LS	Life Safety
CP	Collapse Prevention
C	C
D	D
E	E

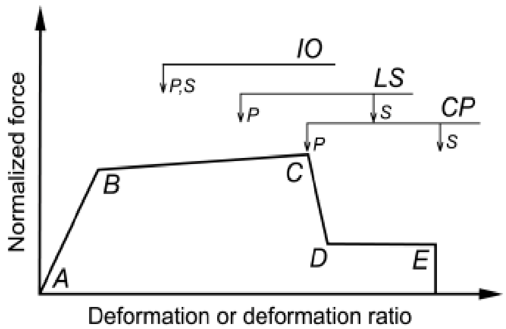

Figure 7. Force–Displacement Relationship of Plastic Hinge (FEMA 356 [9])

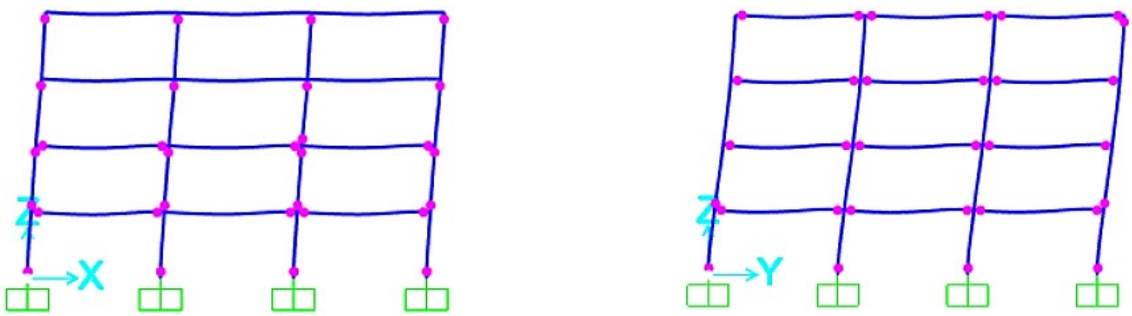

(a) (b)

Figure 8. Plastic Damages in 4-Story Buildings subjected to El Centro–BDE: (a) FBD, (b) DDBD

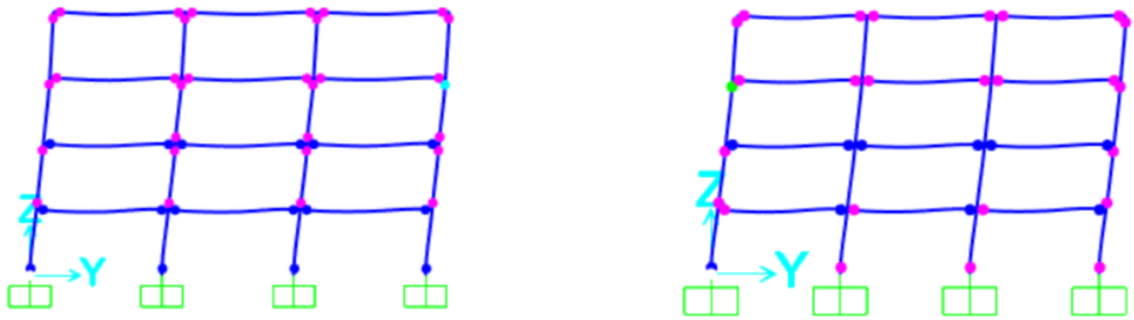

(a) (b)

Figure 9. Plastic Damages in 4-Story Buildings subjected to El Centro–MCE_R: (a) FBD, (b) DDBD

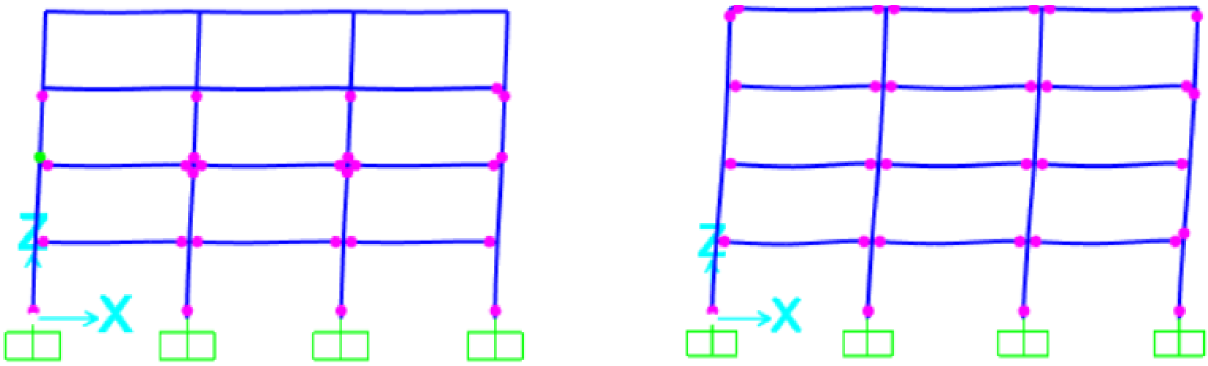

(a) (b)

Figure 10. Plastic Damages in 4-Story Buildings subjected to Kobe–BDE: (a) FBD, (b) DDBD

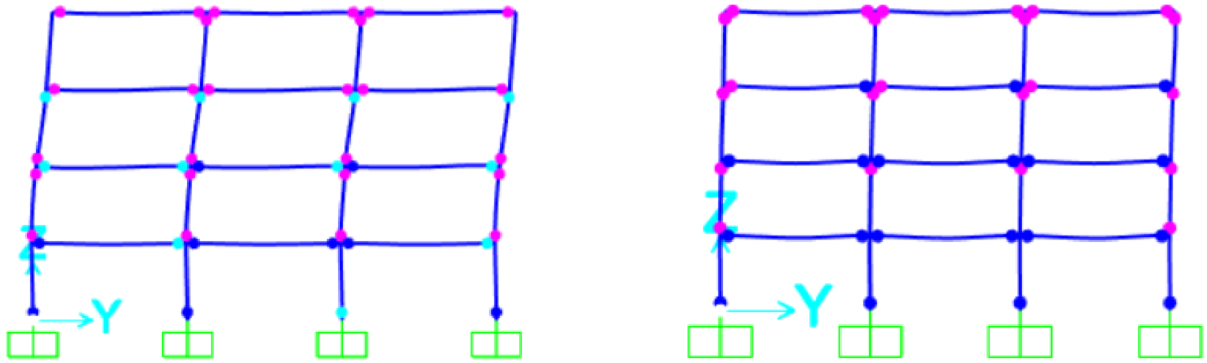

(a) (b)

Figure 11. Plastic Damages in 4-Story Buildings subjected to Kobe–MCE_R: (a) FBD, (b) DDBD

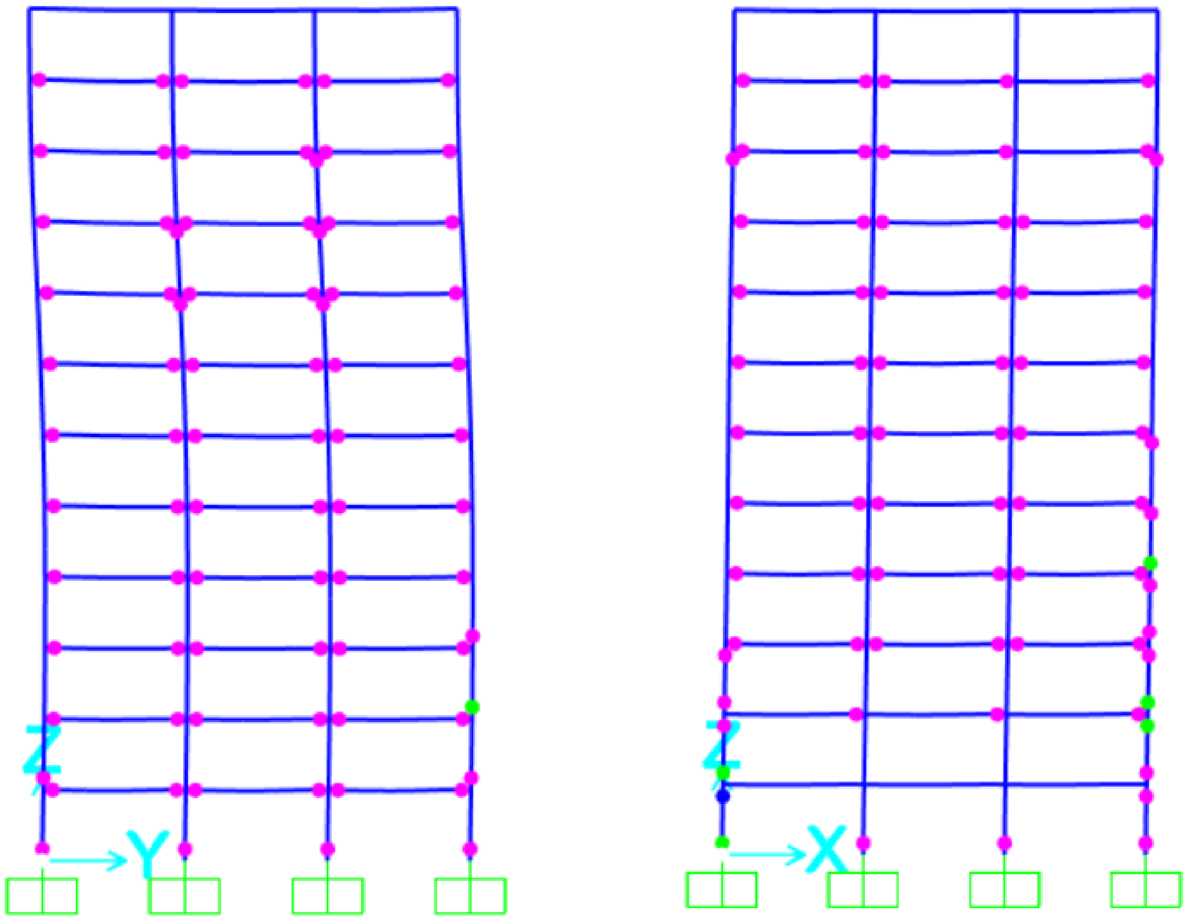

(a) (b)

Figure 12. Plastic Damages in 12-Story Buildings subjected to El Centro–BDE: (a) FBD, (b) DDBD

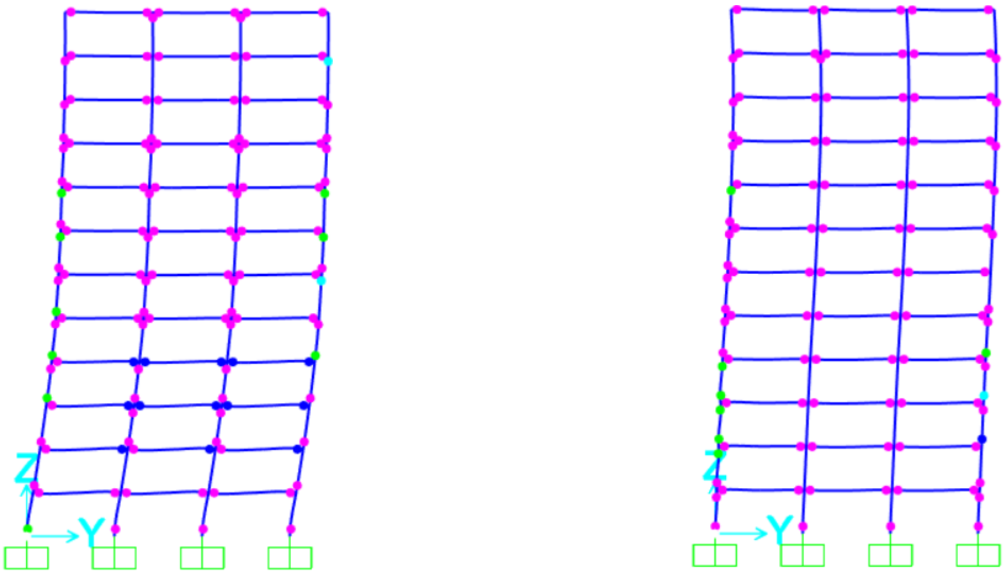

(a) (b)

Figure 13. Plastic Damages in 12-Story Buildings subjected to El Centro–MCE$_R$: (a) FBD, (b) DDBD

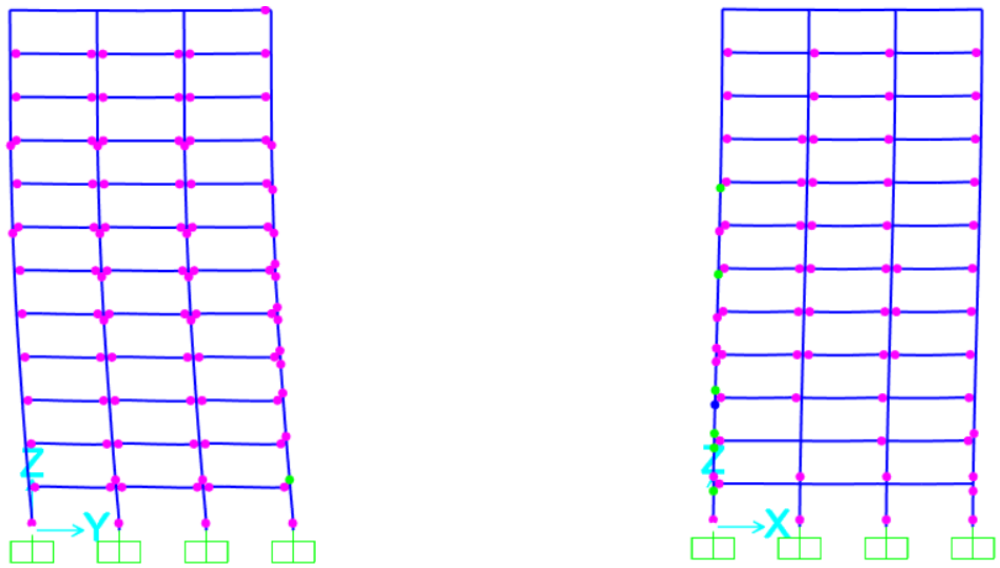

(a) (b)

Figure 14. Plastic Damages in 12-Story Buildings subjected to Kobe–BDE: (a) FBD, (b) DDBD

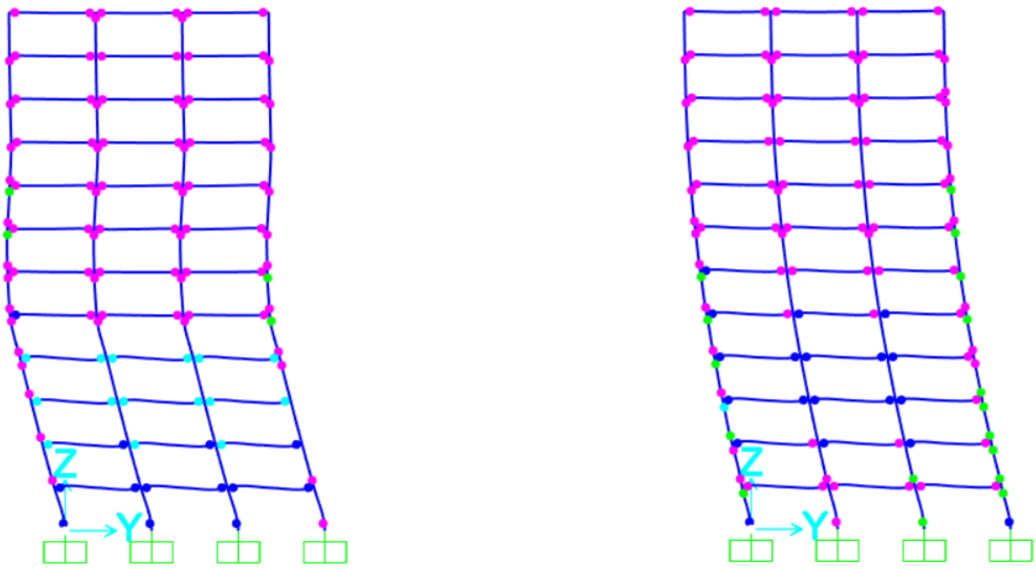

(a) (b)

Figure 15. Plastic Damages in 12-Story Buildings subjected to Kobe–MCE$_R$: (a) FBD, (b) DDBD

Table 11. Buildings' Performance (El Centro Earthquake)

Building	El Centro					
	BDE			MCE_R		
	Mechanism	Damage Level	Drift Ratio	Mechanism	Damage Level	Drift Ratio
4-FBD	X	OK	OK	X	OK	OK
4-DDBD	X	OK	OK	X	X	OK
12-FBD	X	X	OK	X	X	OK
12-DDBD	X	X	OK	X	X	OK

Table 12. Buildings' Performance (Kobe Earthquake)

Building	Kobe					
	BDE			MCE_R		
	Mechanism	Damage Level	Drift Ratio	Mechanism	Damage Level	Drift Ratio
4-FBD	X	X	OK	X	OK	OK
4-DDBD	X	OK	OK	X	X	OK
12-FBD	X	X	OK	X	X	OK
12-DDBD	X	X	OK	X	X	OK

CONCLUSIONS

Based on this study case of regular 4-story and 12-story buildings designed using the FBD and DDBD approaches, it can be concluded that:

1. Buildings designed using both methods have actual drifts that differ from the target of 2%.
   a. In the FBD method, it was expected that the actual drift would be close to the target drift of 2% at the MCE_R earthquake level. However, the actual drift values for both buildings at the MCE_R earthquake level exceeded the target drift. Nevertheless, all drift values remained within the maximum allowable limits at both the BDE and MCE_R earthquake levels. It should also be noted that in the FBD method, buildings are designed based on BDE, which is 2/3 of the MCE_R.
   b. In the DDBD method, it was expected that the actual drift value is close to the target drift of 2% at the BDE earthquake level. However, the actual drift values for the 4-story and 12-story buildings were significantly lower than the target drift of 2%. Even at the MCE_R earthquake level, the actual drift values remained below the 2% target. This means that in terms of drift ratio, the DDBD approach is quite conservative.
2. All buildings, both 4-story and 12-story, designed using the FBD and DDBD approaches, did not experience collapse due to the El Centro or Kobe earthquakes at the MCE_R level. Plastic damages were generally more severe in buildings designed using the FBD approach, with beams and columns experiencing the Collapse Prevention and Life Safety stages. For buildings designed using the DDBD approach, columns also reached the Collapse Prevention stage, although in fewer numbers, while beams only reached the Immediate Occupancy stage.
3. The performance differences observed in points 1 and 2 can be attributed to the distinct design processes inherent to the two approaches, as outlined in Table 2.
4. Despite the intended design for a safe beam-side sway mechanism, all buildings in this study experienced plastic damage at locations beyond the expected beam ends and first-floor columns. This highlights the limitation of the strong column-weak beam concept in the code, that it is not sufficient to provide 100% assurance that the columns are free from plastic damage as expected [16-20].

REFERENCES

1. Chandra, J., Lokito, V.N., and Tambuna, J.A., Seismic Performance of Precast Concrete Special Moment Frames with Hybrid Connection System in Five and Ten Story Buildings, *Civil Engineering Dimension*, *25*(2), 2023, pp. 85–95.
2. Pudjisuryadi, P., Lumantarna, B., Wijaya, F., Aphrodita, C., Jesica, A., Karyanto, Y., and Theodora, M., Application of Modified-Partial Capacity Design Method on 6- and 15-story Square Buildings with Variation in Number of Elastic Columns, *Civil Engineering Dimension*, *24*(1), 2022, pp. 46–53.
3. Pudjisuryadi, P., Wijaya, F., Tanuwijaya, R., Prasetyo, B., and Lumantarna, B., Performance of Six- and Ten-story Reinforced Concrete Buildings Designed by using Modified Partial Capacity Design (M-PCD) Method with 70% Shear Force Ratio, *Civil Engineering Dimension*, *23*(2), 2021, pp. 131–137.
4. Badan Standardisasi Nasional, SNI-03-1726-2019 Tata Cara Perencanaan Ketahanan Gempa untuk Struktur Bangunan Gedung dan Non Gedung, Jakarta, 2019.

5. Lumantarna, E., Lam, N., and Wilson, J., Seismic Assessment of Structures in Regions of Low to Moderate Seismicity, *Civil Engineering Dimension*, *14*(3), 2012, pp. 156–165.
6. Andriono, T., Abraham, A., David A.T.L., and Tjong, W.F., Aplikasi Konsep Berbasis Perpindahan pada Perencanaan Pilar Beton Bertulang untuk Struktur Jembatan, *Civil Engineering Dimension*, *4*(2), 2004, pp. 51–59.
7. Priestley, M., Calvi, G., and Kowalsky, M., *Displacement-based Seismic Design of Structure*, Pavia: IUSS Press, 2007.
8. Şadan, O.B., Petrini, L., and Calvi, G.M., Direct Displacement-based Seismic Assessment Procedure for Multi-Span Reinforced Concrete Bridges with Single-Column Piers, *Earthquake Engineering and Structural Dynamics*, *42*(7), 2013, pp. 1031–1051. https://doi.org/10.1002/eqe.2257
9. Cademartori, M., Sullivan, T.J., and Osmani, S., Displacement-based Assessment of Typical Italian RC Bridges, *Bulletin of Earthquake Engineering*, *18*(9), 2020, pp. 4299–4329. https://doi.org/10.1007/s10518-020-00861-9
10. Dong, W., Li, M., Sullivan, T., MacRae, G., Lee, C.L., and Chang, T., Direct Displacement-based Seismic Design of Glulam Frames with Buckling Restrained Braces, *Journal of Earthquake Engineering*, *27*(8), 2022, pp. 2166-2197. https://doi.org/10.1080/13632469.2022.2110999
11. Chikmath, C., Kamatchi, P., and Vasanwala, S.A., Application of Direct Displacement based Design of Reinforced Concrete Frames Subjected to Earthquake Loads, *International Journal of Recent Technology and Engineering (IJRTE), 8*(5), 2020, pp. 5153–5160. https://doi.org/10.35940/ijrte.e6220.018520
12. Muljati, I., Asisi, F., and Willyanto, K., Performance of Force Based Design Versus Direct Displacement based Design in Predicting Seismic Demands of Regular Concrete Special Moment Resisting Frames, *Procedia Engineering*, Elsevier Ltd., 125, 2015, pp. 1050–1056. https://doi.org/10.1016/j.proeng.2015.11.161
13. Badan Standardisasi Nasional, SNI-03-1727-2020: *Beban Desain Minimum dan Kriteria Terkait untuk Bangunan Gedung dan Struktur Lain*, Jakarta, 2020.
14. Pacific Earthquake Engineering Research Center, *PEER Ground Motion Database El Centro 1940*, 2021. https://ngawest2.berkeley.edu/
15. Federal Emergency Management Agency 356, *Prestandard and Commentary for the Seismic Rehabilitation of Buildings*, Washington, D.C., USA, 2000.
16. Sakai, K. and Sheikh, S.A., What Do We Know about Confinement of Reinforced Concrete Columns? (A Critical Review of Previous Work and Concrete Provisions), *ACI Structural Journal*, *86*(2), 1989, pp. 192-207.
17. Moehle, J.P. and Hooper, J.D., *Seismic Design of Reinforced Concrete Special Moment Frames: A Guide for Practicing Engineers*, Second edition, GCR 16-917-40, Applied Technology Council and Consortium of Universities for Research in Earthquake Engineering, Gaithersburg, 2016.
18. Pudjisuryadi, P. and Lumantarna, B., Kinerja Sistem Rangka Pemikul Momen Khusus Sesuai Sni 03-2847-2002 Ditinjau dari Ketentuan Sengkang Minimum Kolom, *Proceedings of the Konferensi Nasional Teknik Sipil I (KoNTekS I)*, Yogyakarta, Indonesia, May 11-12, 2007, pp. 349-356.
19. Lumantarna, B., Pudjisuryadi, P., Adinata, M.C., and Doly, F.R., Seismic Performance of Special Moment Resisting Frames Designed in Accordance to the Indonesian Concrete and Earthquake Codes, *Proceedings of the 1st International Conference on Modern Design, Construction and Maintenance of Structures*, Hanoi, Vietnam, December 10-11, 2007.
20. Pudjisuryadi, P. and Lumantarna, B., Evaluation of Colums' Flexural Strength of Special Moment Resisting Frame in Accordance to the Indonesian Concrete and Earthquake Codes, *Proceedings of the International Conference on Earthquake Engineering and Disaster Mitigation*, Jakarta, Indonesia, April 14-15, 2008, pp. 591-599.